

RESEARCH ARTICLE SUMMARY

SYNTHETIC BIOLOGY

Synthetic cytokine circuits that drive T cells into immune-excluded tumors

Greg M. Allen, Nicholas W. Frankel, Nishith R. Reddy, Hersh K. Bhargava, Maia A. Yoshida, Sierra R. Stark, Megan Purl, Jungmin Lee, Jacqueline L. Yee, Wei Yu, Aileen W. Li, K. Christopher Garcia, Hana El-Samad, Kole T. Roybal, Matthew H. Spitzer, Wendell A. Lim*

INTRODUCTION: Many solid tumors fail to respond to T cell therapies because their immunosuppressive microenvironment blocks T cell infiltration, activation, and proliferation. Major tumor suppression mechanisms include inhibition of T cell receptor (TCR) signaling and consumption of inflammatory cytokines. Overcoming the suppressive tumor microenvironment remains a major barrier to solid tumor immunotherapy.

RATIONALE: Supplementing T cell activity with inflammatory cytokines, such as high-dose Interleukin-2 (IL-2) has long been known to drive potent antitumor function. Systemic IL-2 treatment, however, has proven prohibitively toxic by causing severe adverse effects including capillary leak syndrome and eventually end-organ dysfunction. Cell autonomous cytokine production has the potential to overcome these toxicities by delivering cytokine locally and directly to a tumor. We engineer therapeutic T cells bearing synthetic cytokine circuits in which a tumor-specific synthetic Notch (synNotch) receptor drives IL-2 production. These tumor-targeted IL-2 delivery circuits offer a potential way to locally overcome tumor suppression while minimizing systemic IL-2 toxicity.

RESULTS: We observed that engineered synNotch→IL-2 induction circuits drove potent infiltration of chimeric antigen receptor (CAR) or TCR T cells into immune-excluded tumor models of pancreatic cancer and melanoma. This improved infiltration was associated with significantly improved tumor clearance and survival in these challenging immune-competent tumor models. Unlike systemically delivered IL-2, the local cell-based IL-2 circuit does not show toxicity as these synNotch→IL-2 circuits are not dependent on TCR/CAR activation but are still tumor-targeted.

However, the exact mechanism used to deliver IL-2 proved to be critical. CAR T cells with SynNotch-induced IL-2 circuits led to far better antitumor efficacy compared with CAR T cells engineered with constitutive IL-2 expression or TCR/CAR-induced IL-2 expression (e.g., from an nuclear factor of activated T cells (NFAT) promoter). Furthermore, we found that autocrine production of IL-2, where the same T cell expresses the CAR/TCR and synNotch→IL-2 circuit, proved to be critical. Paracrine delivery of IL-2, where a CAR T cell is supported by a separate T cell with a synNotch→IL-2 circuit, proved ineffective in the presence of competing native IL-2 consumer cells, such as host regulatory T cells or bystander T cells.

High-dimensional immune profiling shows that the IL-2 synthetic cytokine circuits act primarily on T cell populations without causing significant changes to other immune cell compartments. The tumors show significantly increased infiltration of both the CAR T cells and host bystander T cells. Nonetheless, only the antitumor CAR T cells show enhanced markers of activation, proliferation, and cytotoxicity, as well as reduced markers of exhaustion.

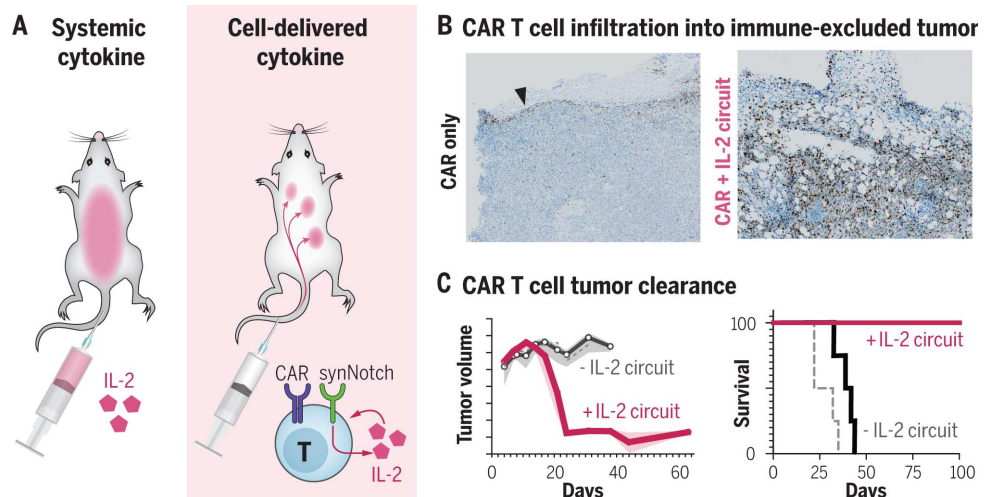
We hypothesize that these circuits are effective because they bypass requirements for TCR/CAR activation and provide IL-2 in a more potent autocrine configuration. These features thereby allow the engineered T cell to overcome the main modes of tumor immune suppression: inhibition of TCR signaling and competitive cytokine consumption. These engineered T cells appear to act as pioneers, triggering expansion in the tumor through their synNotch-induced IL-2 production, which then cooperatively enables the initiation of sustained CAR/TCR-mediated T cell activation and killing.

CONCLUSION: These results show that it is possible to reconfigure T cell circuits to reconstitute the key outputs required for a robust antitumor response (CAR/TCR activation and inflammatory cytokine signaling), but in a manner that bypasses the critical points of tumor immune suppression. These types of engineered local cytokine delivery circuits may thereby provide a potential general strategy for driving effective T cell activity against immune-suppressed solid tumors. ■

The list of author affiliations is available in the full article online.
*Corresponding author. Email: wendell.lim@ucsf.edu
Cite this article as G. M. Allen et al., *Science* 378, eaba1624 (2022). DOI: [10.1126/science.aba1624](https://doi.org/10.1126/science.aba1624)

S READ THE FULL ARTICLE AT
<https://doi.org/10.1126/science.aba1624>

Therapeutic T cells engineered with tumor-triggered IL-2 production infiltrate and clear immune-excluded tumors. (A) We hypothesized that cell autonomous cytokine delivery will allow for, safer, more effective delivery of key inflammatory cytokines like IL-2. Specifically, IL-2 induction circuits that utilize synNotch to bypass requirements for CAR/TCR activation and provide IL-2 in an autocrine configuration allow CAR T cells to operate in immunosuppressive tumor micro-environments. (B) T cell infiltration into tumors, where addition of IL-2 induction circuit substantially improves T cell infiltration into otherwise immune-excluded tumor micro-environments. (C) CAR T cells with an IL-2 induction circuit (pink) are able to clear pancreatic cancer tumors that are otherwise refractory to standard CAR T cell treatments (black).



RESEARCH ARTICLE

SYNTHETIC BIOLOGY

Synthetic cytokine circuits that drive T cells into immune-excluded tumors

Greg M. Allen^{1,2,†}, Nicholas W. Frankel^{1,3,†}, Nishith R. Reddy^{1,3}, Hersh K. Bhargava^{1,4}, Maia A. Yoshida^{1,3}, Sierra R. Stark^{1,3}, Megan Puri^{1,3}, Jungmin Lee^{1,3}, Jacqueline L. Yee⁵, Wei Yu^{1,3}, Aileen W. Li^{1,3}, K. Christopher Garcia⁶, Hana El-Samad^{1,7}, Kole T. Roybal^{1,5,8}, Matthew H. Spitzer^{5,8,9}, Wendell A. Lim^{1,3,7,8,*}

Chimeric antigen receptor (CAR) T cells are ineffective against solid tumors with immunosuppressive microenvironments. To overcome suppression, we engineered circuits in which tumor-specific synNotch receptors locally induce production of the cytokine IL-2. These circuits potently enhance CAR T cell infiltration and clearance of immune-excluded tumors, without systemic toxicity. The most effective IL-2 induction circuit acts in an autocrine and T cell receptor (TCR)- or CAR-independent manner, bypassing suppression mechanisms including consumption of IL-2 or inhibition of TCR signaling. These engineered cells establish a foothold in the target tumors, with synthetic Notch-induced IL-2 production enabling initiation of CAR-mediated T cell expansion and cell killing. Thus, it is possible to reconstitute synthetic T cell circuits that activate the outputs ultimately required for an antitumor response, but in a manner that evades key points of tumor suppression.

Chimeric antigen receptor (CAR) T cells have demonstrated remarkable success in the treatment of B cell malignancies (1, 2). Nonetheless, application of CAR or T cell receptor (TCR)-engineered T cells to solid tumors has proven far more challenging (3). Many solid tumors create an immune-excluded local microenvironment that blocks the infiltration, activation, or expansion of cytotoxic T cells (4). Within this tumor microenvironment, activation of CAR/TCR pathways are inhibited by local immunosuppressive factors and cells (5–7). While evidence suggests that local administration of high-dose inflammatory cytokines could help reverse tumor suppression (8), combining adoptively transferred T cells with systemic cytokine administration or engineered cytokine production has shown either systemic toxicity or poor ef-

ficacy (9–11). There is a clear need to engineer next-generation therapeutic T cells with an enhanced ability to overcome tumor suppression, without exacerbating off-target or systematic toxicity.

We have created synthetic cytokine circuits as a strategy to improve therapeutic T cell activity against immune-excluded solid tumors. Using the recently developed synthetic Notch (synNotch) receptor (12, 13), we have created a bypass signaling pathway in which tumor recognition by synNotch induces local interleukin-2 (IL-2) production (Fig. 1A). The inflammatory cytokine IL-2 plays a critical role as both an output of T cell activation and as a promoter of T cell activation and expansion (14–17). Suppressive tumor microenvironments can both reduce IL-2 production and/or competitively consume IL-2 (18–20). Thus, we hypothesized that providing IL-2 in a tumor-targeted but TCR/CAR-independent manner could help bypass tumor immune suppression. Indeed, we find that certain synthetic IL-2 circuits drive highly efficient CAR T cell infiltration and tumor control in immune-excluded solid tumor models, without concomitant systemic or off-target toxicity. Immune profiling shows expansion of CAR T cells only within the tumor, with increased markers of activation and decreased markers of exhaustion. Synthetic IL-2 production likely enables infiltrating T cells to survive and initiate sustained CAR-mediated activation, expansion, and tumor killing. This type of synthetic cytokine delivery circuit could provide a powerful general approach for remodeling and overcoming immunosuppressive solid tumors.

Engineering synthetic IL-2 circuits that drive local T cell proliferation independent of T cell activation

To design a tumor-induced synthetic IL-2 circuit in T cells, we used a synNotch sensor to induce the transcription of an IL-2 transgene (Fig. 1B). In essence, synNotch receptors are chimeric receptors with a variable extracellular recognition domain, a Notch-based cleavable transmembrane domain, and an intracellular transcriptional domain (12, 13). Antigen binding induces intramembrane receptor cleavage, releasing the transcriptional domain to enter the nucleus and promote expression of a target transgene.

We built a prototype circuit in primary human T cells using a synNotch receptor that recognizes the model antigen CD19, combined with a synNotch-responsive promoter driving expression of human IL-2 or an affinity-enhanced variant of IL-2 (known as super-2 or sIL-2) (21). As intended, stimulation of the synNotch receptor in vitro induced strong proliferation of the engineered cell population (Fig. 1C). Cells with the anti-CD19 synNotch→sIL-2 circuit could function in a paracrine manner, driving the proliferation of co-cultured nonengineered T cells (Fig. 1D) or natural killer cells (Fig. 1E) in vitro. The degree of proliferation was dependent on the type of gamma-chain cytokine payload, with significant T cell proliferation seen with production of either IL-2 or sIL-2 (Fig. 1D). Production of the homeostatic cytokine IL-7 (22) led to T cell survival with minimal expansion whereas untethered IL-15 (23) had no effect. Thus, in vitro, a synNotch→sIL-2 circuit T cell can drive its own proliferation, as well as the proliferation of other co-cultured IL-2 responsive cells.

We then tested whether the synNotch→sIL-2 circuit could drive targeted expansion of human T cells in vivo, independent of CAR or TCR activation. We established a bilateral K562 tumor model in immunocompromised Non-obese diabetic *scid* gamma (NSG) mice, where only one flank tumor expressed the synNotch target antigen, CD19 (Fig. 1E). Human primary CD8+ T cells engineered with the anti-CD19 synNotch→sIL-2 circuit were tagged with enhanced firefly luciferase (eff-luc) and injected intravenously. Cells with the synthetic IL-2 circuit autonomously identified the target tumor (CD19+/right) and locally expanded by a factor of ~100 within this tumor (Fig. 1E). By contrast, no off-target expansion was seen in the contralateral (CD19-) tumor. Flow cytometry analysis of tumor infiltrating lymphocytes in the target and off-target tumor showed synNotch activation, T cell expansion, and proliferation only in the CD19+ tumor (Fig. S2, A to C). The administered T cells had no CAR or TCR reactivity against tumors and thus the synthetic production of IL-2 alone did not result in killing of the K562 tumors in this immunodeficient NSG mouse model (Fig. S2D).

¹Cell Design Institute; University of California San Francisco, San Francisco, CA 94158, USA. ²Department of Medicine, University of California San Francisco; San Francisco, CA 94158, USA. ³Department of Cellular and Molecular Pharmacology, University of California San Francisco; San Francisco, CA 94158, USA. ⁴Biophysics Graduate Program, University of California San Francisco; San Francisco, CA 94158, USA. ⁵Department of Microbiology and Immunology, University of California San Francisco; San Francisco, CA 94158, USA. ⁶Department of Molecular and Cellular Physiology and Structural Biology, Howard Hughes Medical Institute, Stanford University; Stanford, USA. ⁷Department of Biochemistry and Biophysics, University of California San Francisco; San Francisco, CA 94158, USA. ⁸Parker Institute for Cancer Immunotherapy, University of California San Francisco; San Francisco, CA 94158, USA. ⁹Department of Otolaryngology-Head and Neck Surgery, University of California San Francisco; San Francisco, CA 94158, USA.

*Corresponding author. Email: wendell.lim@ucsf.edu

†These authors contributed equally to this work.

Fig. 1. Synthetic synNotch→IL-2 circuits can drive local T cell proliferation independent of TCR activation or cooperatively with T cell killing.

(A) The tumor microenvironment (TME) acts to suppress T cell activation, including inflammatory cytokine (e.g., IL-2) production. To bypass suppression we propose engineering synthetic IL-2 circuits triggered by tumor antigens in a manner independent from TCR/CAR activation.

(B) Synthetic IL-2 circuits were created in human primary T cells using anti-CD19 synNotch receptors to drive production of an inflammatory cytokine (super IL-2 or sIL-2). IL-2 is produced only when stimulated by A375 tumor cells bearing the cognate CD19 antigen; compare with fig. S1A. **(C)** The synthetic IL-2 circuit drives autocrine proliferation of primary human T cells *in vitro* only when the circuit is triggered (here, myc-tagged synNotch is activated by anti-myc antibody-coated beads).

(D) Synthetic IL-2 circuit signals in a paracrine fashion to stimulate proliferation of a bystander population of human T cells that lack a synthetic circuit *in vitro*.

For [(C) and (D)] the median is plotted; shading shows SEM ($n = 3$) and filled markers indicate significant expansion >1 , right-tailed student's t test, $P < 0.05$.

Additional replicates of autocrine and paracrine proliferation are shown in fig. S1B.

(E) Dual flank tumor model in NSG mice to monitor T cell trafficking *in vivo*. Primary human T cells were engineered with synthetic anti-CD19→sIL-2 circuit and eff-luc (to track cells) and administered to mice engrafted with CD19⁺ (right) and CD19⁻ (left) K562 tumors.

Example bioluminescence imaging shown 7 days after T cell injection. Circles indicate tumors (blue, white) and spleen (red). Plot shows quantification of T cell luminescence over time for CD19⁺ and CD19⁻ tumors. Dashed line shows T cells in CD19⁺ tumors with no circuit added; shading shows SEM.

(F) Tumor-reactive T cells, such as those bearing an anti-NY-ESO TCR, fail to produce effective cytokine and killing responses against antigen-positive tumors. We hypothesize that simultaneously engaging the TCR and a synthetic IL-2 circuit could enhance a local T cell response.

In this case T cells bearing an anti-NY-ESO TCR and an anti-membrane-bound GFP (mGFP) synNotch→sIL-2 circuit could function as an AND gate that requires two antigen inputs to stimulate tumor killing, allowing more precise recognition strategies.

Here a two-flank A375 tumor model in NSG mice, with NY-ESO only (left) and NY-ESO/GFP (right), was generated. Plots show tumor growth over time. Both autocrine and paracrine forms of the TCR + anti-GFP synNotch→sIL-2 cells show significantly enhanced control of only the dual antigen tumor.

Error shading: SEM Dashed line indicates dual antigen tumor growth curve with no T cell treatment. NY-ESO TCR-only control and individual tumor growth curves available in fig. S4.

Both autocrine and paracrine forms of the TCR + anti-GFP synNotch→sIL-2 cells show significantly enhanced control of only the dual antigen tumor.

Error shading: SEM Dashed line indicates dual antigen tumor growth curve with no T cell treatment. NY-ESO TCR-only control and individual tumor growth curves available in fig. S4.

Both autocrine and paracrine forms of the TCR + anti-GFP synNotch→sIL-2 cells show significantly enhanced control of only the dual antigen tumor.

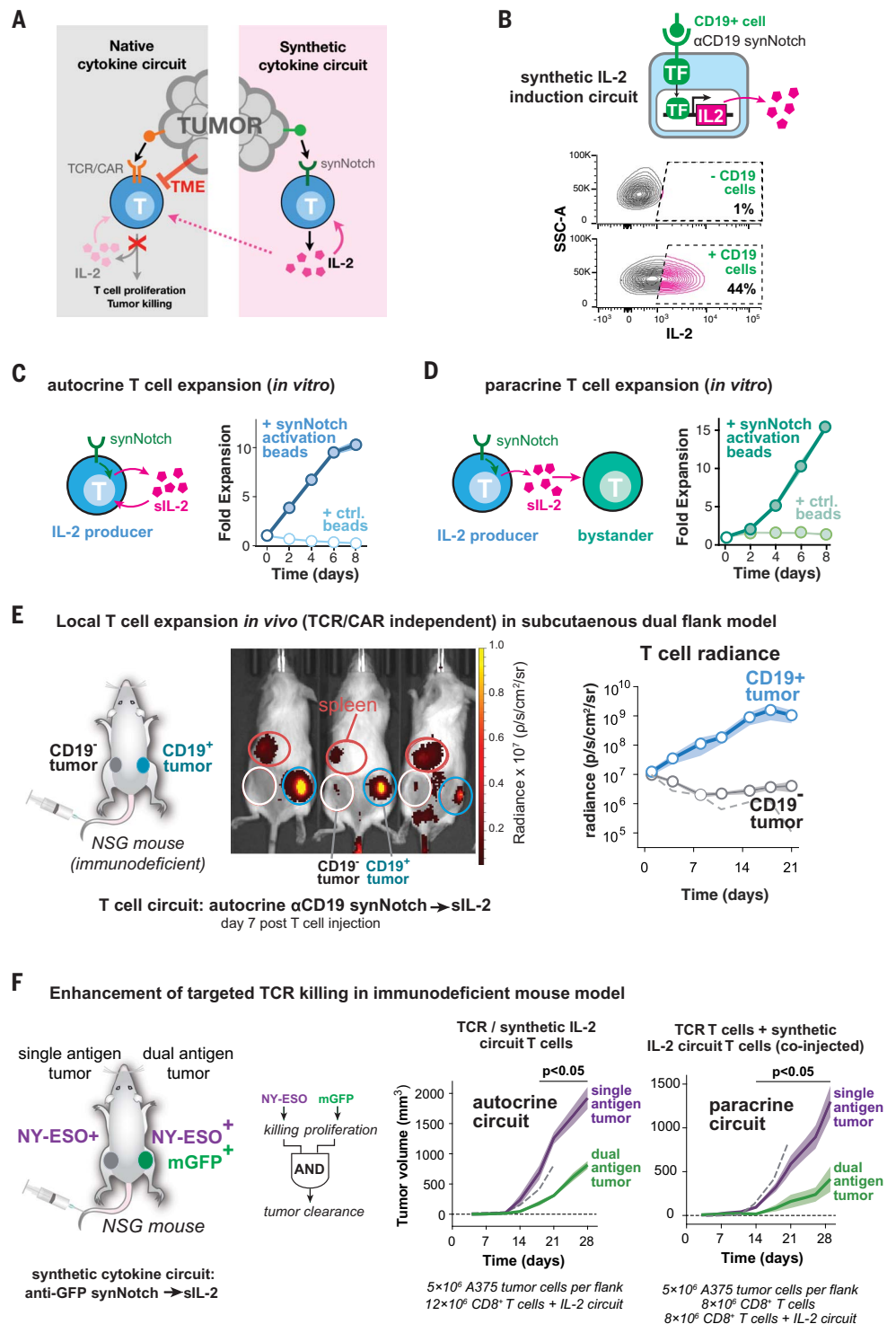
Error shading: SEM Dashed line indicates dual antigen tumor growth curve with no T cell treatment. NY-ESO TCR-only control and individual tumor growth curves available in fig. S4.

Error shading: SEM Dashed line indicates dual antigen tumor growth curve with no T cell treatment. NY-ESO TCR-only control and individual tumor growth curves available in fig. S4.

Error shading: SEM Dashed line indicates dual antigen tumor growth curve with no T cell treatment. NY-ESO TCR-only control and individual tumor growth curves available in fig. S4.

Error shading: SEM Dashed line indicates dual antigen tumor growth curve with no T cell treatment. NY-ESO TCR-only control and individual tumor growth curves available in fig. S4.

Error shading: SEM Dashed line indicates dual antigen tumor growth curve with no T cell treatment. NY-ESO TCR-only control and individual tumor growth curves available in fig. S4.



We also found that the anti-CD19 synNotch→sIL-2 circuit was also capable of driving T cell expansion in a paracrine (two-cell type) configuration in this NSG mouse model. We co-

injected a population of bystander T cells, which did not express the sIL-2 induction circuit but expressed luciferase to distinguish them from the synNotch→sIL-2 T cells. Co-

injected into mice at a 1:1 ratio, the bystander cells also specifically expanded in the targeted (CD19⁺/right) tumor (fig. S3, A to D), where the synNotch receptor was locally activated

(fig. S3E). This paracrine T cell expansion was not observed in negative control experiments using synNotch T cells that either did not produce sIL-2 or did not recognize CD19 (fig. S3F). In summary, this work represents one of the first examples in which locally targeted T cell expansion can be induced in a manner uncoupled from TCR or CAR activation.

Synthetic IL-2 circuits can enhance targeted T cell cytotoxicity in vivo

Many engineered T cell therapies show effective cytotoxicity in vitro but fail to show sufficient proliferation or persistence to achieve effective tumor control in vivo. For example, cells bearing the affinity-enhanced anti-NY-ESO-1 TCR are able to lyse A375 melanoma tumors in vitro (24) but have shown limited clinical benefit in patients or preclinical models (25). We hypothesized that the addition of a synthetic cytokine circuit producing IL-2 might enhance tumor control by NY-ESO-1 T cells. Moreover, these T cells might function as a new type of AND gate (26, 27), where a therapeutic T cell exhibits enhanced specificity by requiring two antigens to be present before triggering its full cytotoxic response: the TCR antigen required for T cell activation, and the synNotch antigen required for inducing IL-2 production. In this case, we used an anti-GFP synNotch→sIL-2 synthetic cytokine circuit. By requiring the presence of both the TCR antigen (NY-ESO-1) and the synNotch antigen (in this case, membrane-tethered green fluorescent protein (GFP)) (Fig. 1F), this cellular design strategy should further minimize off-target toxicity.

We examined the efficacy of anti-NY-ESO-1 TCR human T cells in NSG mice using a bilateral tumor model of a NY-ESO-1⁺ melanoma (A375). Only one flank tumor was co-labeled with the synNotch-targeted model antigen (membrane-tethered GFP). Anti-NY-ESO-1 TCR-expressing T cells lacking the synthetic IL-2 circuit were largely ineffective at controlling the growth of both the single (NY-ESO⁺) and dual (NY-ESO⁺/GFP⁺) antigen tumors (fig. S4A). However, when mice were treated with T cells simultaneously expressing both the anti-NY-ESO-1 TCR and the anti-GFP synNotch→sIL-2 circuit, the dual-targeted NY-ESO⁺/GFP⁺ tumor now showed a significant reduction in tumor size (Fig. 1F). Similar tumor reduction was observed when IL-2 was provided in a paracrine configuration, by co-injection of one cell type only expressing the anti-NY-ESO-1 TCR and a second cell type only expressing the synthetic IL-2 circuit. Critically, in either the autocrine or paracrine configuration, the synthetic IL-2 circuit did not cause a reduction in the contralateral NY-ESO⁺/GFP⁺ tumor (lacking the synNotch ligand), highlighting the precisely targeted impact of the synthetic IL-2 circuit.

Using luciferase tracking of anti-NY-ESO-1 TCR T cells, we observed substantially increased

intratumoral expansion of T cells only in tumors that were targeted by the synthetic IL-2 circuit (fig. S5A). The synthetic IL-2 circuit was only activated in the targeted double antigen positive tumor (fig. S5B), and we observed a significant increase in T cell activation markers in this targeted tumor (fig. S5C). A synthetic IL-2 circuit T cell without co-delivery of a tumor-reactive cytotoxic T cell population did not produce tumor control in these NSG mouse models (fig. S5D).

Autocrine configuration of the synthetic IL-2 circuit is required in immunocompetent tumor models

Although the above results show that synthetic synNotch→IL-2 circuits can significantly enhance T cell activity and expansion in immunodeficient mouse tumor models, we wanted to test whether they could also be effective in immunocompetent mouse models. Important factors influencing IL-2 production and consumption are likely missing in immunodeficient mouse models. Key missing factors include inhibitors of T cell activation (28) and the presence of competing IL-2 consumer cells (e.g., both native T cells and T regulatory cells), which could significantly lower the effectiveness of synthetically produced IL-2 within tumors (29, 30). To study the effects of local IL-2 production within fully immunocompetent mouse tumor models, we rebuilt our synthetic IL-2 circuit in primary mouse T cells (Fig. 2A). Primary CD3⁺ mouse T cells were engineered to express an anti-human-CD19 synNotch→mouse IL-2 (mIL-2) circuit. This circuit resulted in synNotch-induced proliferation of mouse T cells in vitro, as observed previously with human T cells (fig. S6A).

We then chose to deploy this IL-2 circuit in targeting the mouse pancreatic tumor model KPC (KrasLSL.G12D/+; p53R172H/+; PdxCre/+ (31, 32), as this immune-excluded tumor exhibits the challenging immunotherapy refractory features of pancreatic ductal adenocarcinoma (33). Like most pancreatic ductal adenocarcinomas, these cells express the tumor target antigen mesothelin (34). Although anti-mesothelin mouse CAR T cells show robust cytotoxicity against KPC cells in vitro (fig. S6B), they show limited to no tumor control of KPC tumors in vivo (fig. S6C). Thus, this immune competent mouse model replicates the poor in vivo therapeutic efficacy reported in early phase clinical trials of standard antimesothelin CAR T cells in pancreatic cancer (3), making it an ideal model for testing enhancement of the CAR T cells with synthetic IL-2 circuits. We engineered KPC tumor cells that, in addition to endogenously expressing the CAR antigen (mesothelin), also expressed a model synNotch antigen (human CD19).

We first tested CAR T cell enhancement by a paracrine synNotch→mIL-2 circuit. Anti-

mesothelin CAR T cells were co-injected with a second T cell population expressing the anti-CD19 synNotch→mIL-2 circuit. Distinct from our studies in immunodeficient mice, these paracrine IL-2 circuit cells failed to improve tumor control in an immune competent context (Fig. 2B and fig. S7A). Instead, we found that in this fully immunocompetent tumor model, improved CAR T cell-mediated tumor control was only observed with the autocrine configuration of the synthetic IL-2 circuit—i.e., the cytotoxic receptor (CAR) and the synNotch→IL-2 circuit must be encapsulated within the same cell (Fig. 2C and fig. S7B). We hypothesize that the presence of competing host IL-2 consumer cells (e.g., bystander T cells and T_{regs}) in immune-competent models contributes to this major difference between the autocrine and paracrine circuits (i.e., paracrine circuits might be more sensitive to competing IL-2 sink cells), a model consistent with more in-depth tumor profiling data in later sections of this paper.

The autocrine synthetic IL-2 circuit anti-mesothelin CAR-T cells were extremely potent. In an even more challenging immune-competent mouse model, in which KPC tumors were engrafted orthotopically in the pancreas, complete tumor clearance was observed upon treatment (Fig. 2D): 100% of mice survived, compared with 0% with CAR-only T cells. Simply increasing the dose of anti-mesothelin CAR-T cells had a negligible effect compared to addition of the synthetic IL-2 circuit (fig. S8, A and B).

This type of autocrine IL-2 circuit also shows similar substantial therapeutic improvement in treating a different type of immune-excluded solid tumor: B16-F10 OVA intradermal melanoma tumors, treated with OT-1 TCR-expressing T cells (Fig. 2E and fig. S7C). Here again, OT-1 T cells without the cytokine circuit are ineffective in vivo in immune-competent models (despite in vitro cytotoxic activity; see fig. S6D). Only when the OT-1 TCR is co-expressed with the autocrine synNotch→IL-2 circuit do we observe effective infiltration and tumor clearance in the immune-competent model.

Comparison with other strategies of IL-2 co-delivery

Notably, this strong therapeutic improvement was not observed with other methods of co-delivering IL-2 with CAR T cells. We tested systemic co-administration of IL-2 at maximum-tolerated doses (35) (Fig. 3B and fig. S9B), expression of IL-2 in the CAR T cell from a constitutive promoter (“armored CAR”) (Fig. 3C and fig. S9C), or expression of IL-2 from a T cell-activated promoter such as pNFAT (36) (Fig. 3D and fig. S9D).

Systemically injected IL-2 led to systemic toxicity without improving CAR T cell activity (fig. S10B). Constitutive production of IL-2 was

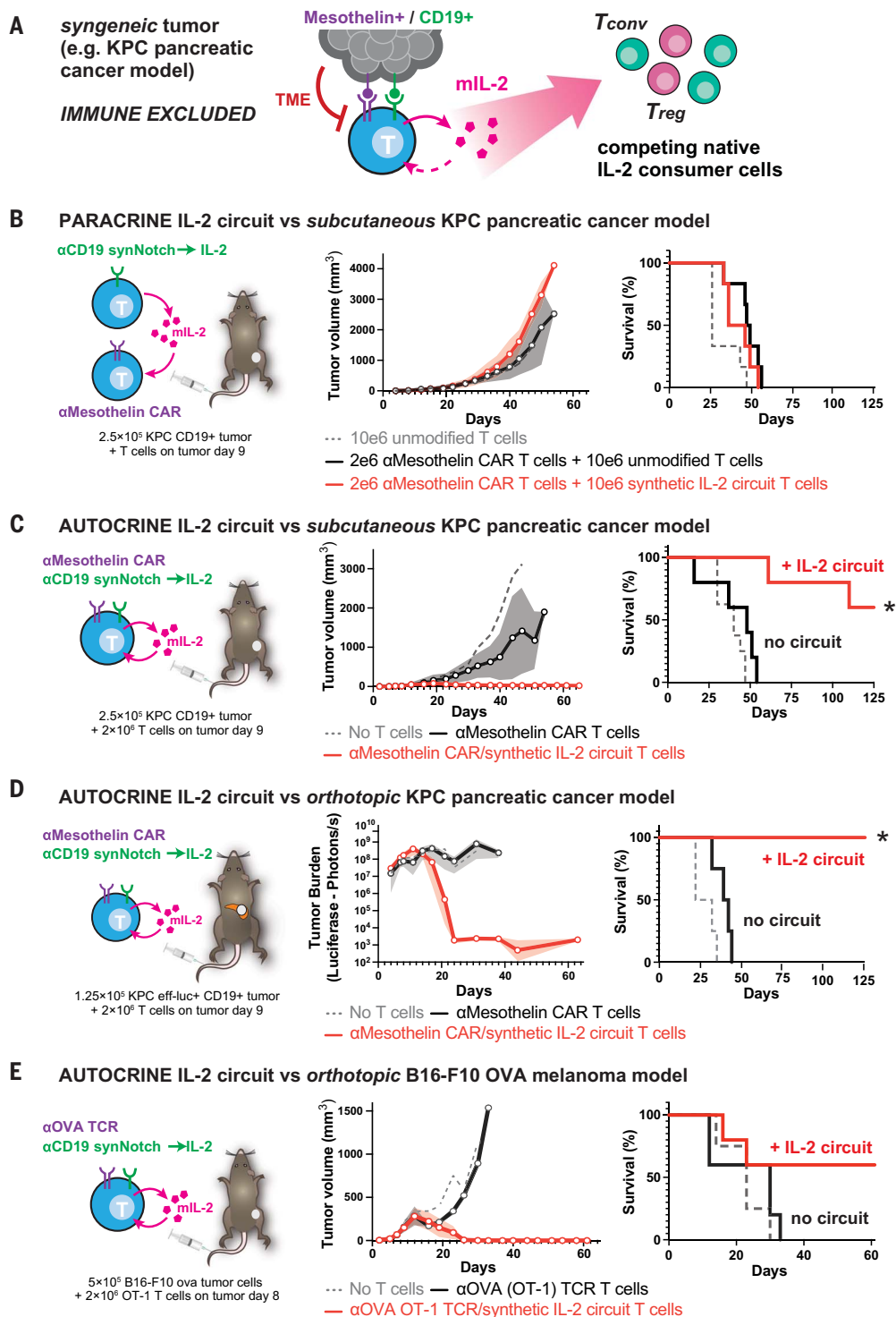
Fig. 2. Autocrine synthetic IL-2 circuits strongly improve T cell cytotoxicity against multiple models of immune-excluded syngeneic tumors.

(A) The synthetic IL-2 circuit was recapitulated in mouse T cells producing mouse IL-2 (mIL-2) to test circuits in the presence of an intact immune system, suppressive TME, and native IL-2 consumer cells.

(B) KPC CD19⁺ pancreatic tumors were engrafted subcutaneously into immunocompetent C57/B16 mice and treated 9 days later with synthetic IL-2 circuit T cells and anti-mesothelin CAR T cells as a two-cell paracrine system. No tumor control was observed in this paracrine configuration, even though KPC tumors express mesothelin.

(C) KPC CD19⁺ pancreatic tumors were engrafted as in (B) and treated 9 days later with T cells engineered with both a synthetic IL-2 circuit and an anti-mesothelin CAR (autocrine configuration). Significant improvement in tumor control was observed (red lines) compared to anti-mesothelin CAR T cells combined with a dummy synthetic cytokine circuit (synNotch only produces BFP, black lines).

(D) KPC CD19⁺ pancreatic tumors were engrafted orthotopically in the pancreas tail and treated 9 days later with engineered T cells. Only with the addition of the IL-2 circuit was 100% survival observed, out to 120 days (duration of study). (E) B16F10 OVA CD19⁺ melanoma tumors were engrafted orthotopically into immunocompetent C57/B16 mice and treated 8 days later with 2×10^6 engineered mouse CD8⁺ OT-1 (anti-OVA) T cells. Tumor control was only observed in mice treated with T cells expressing the IL-2 circuit. For [(B) to (E)] All plots show tumor burden measured by average \pm SEM of caliper or bioluminescence measurements and overall survival ($n = 4$ to 5 per group; *, significant difference in survival with addition of IL-2 circuit using log-rank test, $P < 0.05$). See figs. S7 and S8 for individual growth curves data.



unable to support T cell proliferation *in vitro* (fig. S11A) likely in part due to significant silencing of the constitutive IL-2 transgene (fig. S11B) (37). IL-2 can have a biphasic effect on T cell survival (38), partly because of promotion of activation-induced cell death (39) and T cell differentiation (40). We find that such negative effects are exacerbated by constitutive IL-2 production (fig. S11C). This sug-

gests that when and how the IL-2 cytokine is produced is critical in determining the outcome.

Notably, despite its potent antitumor efficacy, the synNotch \rightarrow IL-2 circuit showed no evidence of systemic cytokine toxicity or exacerbation of CAR T cell toxicity, as assessed by mouse survival, body weight, spleen weight, and measurements of hepatotoxicity (fig. S10).

Moreover, the required recognition of two antigen inputs (CAR and synNotch antigens) should further enhance the specificity of tumor targeting [as seen by specific targeting to dual antigen tumors (fig. S7C) and reduced hepatotoxicity (fig. S10C)]. In summary, combining a tumor-reactive TCR/CAR with an autocrine synNotch \rightarrow IL-2 circuit results in potent and localized antitumor enhancement.

Fig. 3. Synthetic Notch-based cytokine delivery is required for effective control of KPC tumors.

KPC CD19⁺ pancreatic tumors were engrafted subcutaneously into immunocompetent C57/Bl6 mice and treated 9 days later with T cells as labeled. Plotted here is a schematic for IL-2 production as well as overall survival for each cell design compared to matched untreated mice. $n = 4$ to 5 per group. Tumor measurements for each condition are plotted in fig. S9. (A) 1×10^6 anti-mesothelin CAR T cells with no additional IL-2.

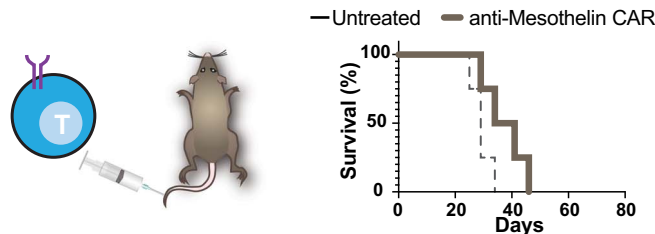
(B) 2×10^6 anti-mesothelin CAR T cells with systemic IL-2 administered at a high dose (250,000 to 750,000 IU/mL) twice daily intraperitoneally for 7 days.

(C) 1×10^6 anti-mesothelin CAR T cells engineered to constitutively express mIL-2 using a PGK promoter.

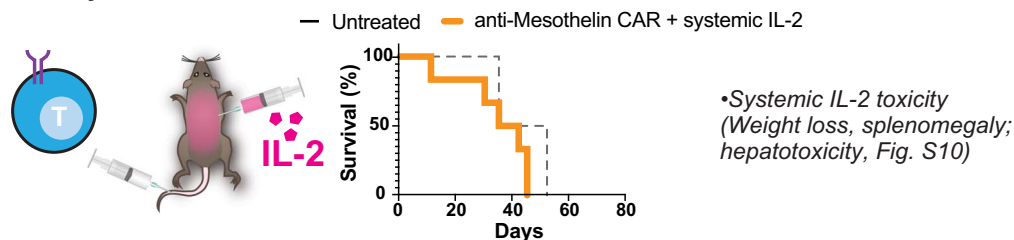
(D) 1×10^6 anti-mesothelin CAR T cells engineered to inducibly express mIL-2 under the control of an NFAT promoter.

(E) 1×10^6 anti-mesothelin CAR T cells engineered to inducibly express mIL-2 under the control of an anti-CD19 synNotch.

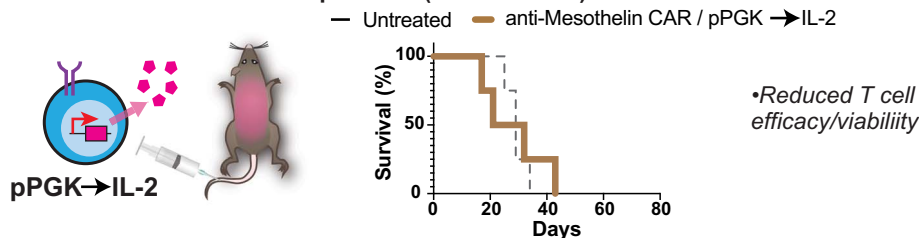
A CAR T cell without additional IL-2



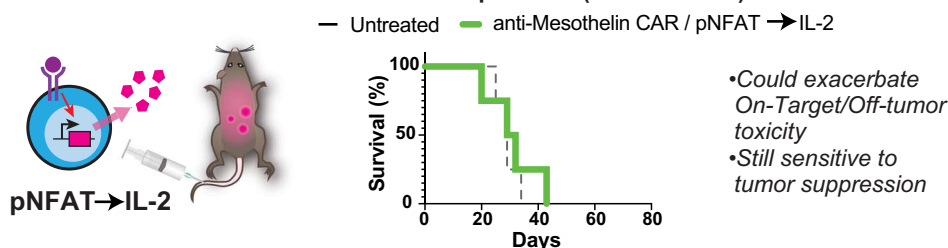
B CAR T + Systemic IL-2 administration



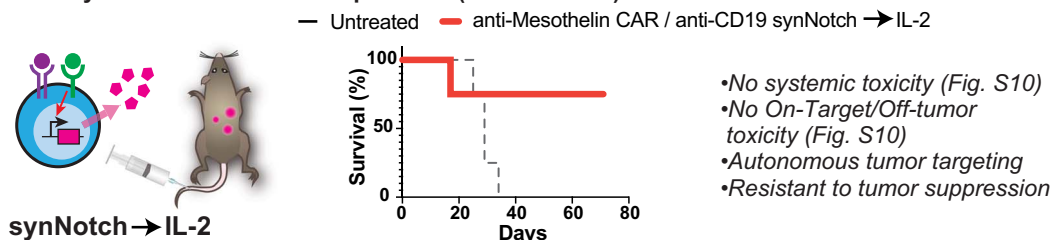
C CAR T + Constitutive IL-2 expression (cell delivered)



D CAR T + TCR/CAR activation induced IL-2 expression (cell delivered)



E CAR T + synNotch induced IL-2 expression (cell delivered)



The synthetic IL-2 circuit drives T cell infiltration into immune-excluded tumors

To better characterize how this autocrine synthetic IL-2 circuit improves CAR T cell control of syngeneic pancreatic tumor models, we profiled the tumors in more depth during treatment. We collected KPC pancreatic tumor specimens at the beginning and partway into tumor regression (8 and 23 days after T cell

treatment, respectively), and measured CD3⁺ T cell infiltration using immunohistochemistry. Tumors treated with standard anti-mesothelin CAR T cells displayed a classic immune-excluded phenotype, with very limited T cell infiltration inside the tumor core and most T cells gathered at the tumor periphery (Fig. 4, top). By contrast, tumors treated with CAR T cells containing the synthetic autocrine IL-2 circuit showed

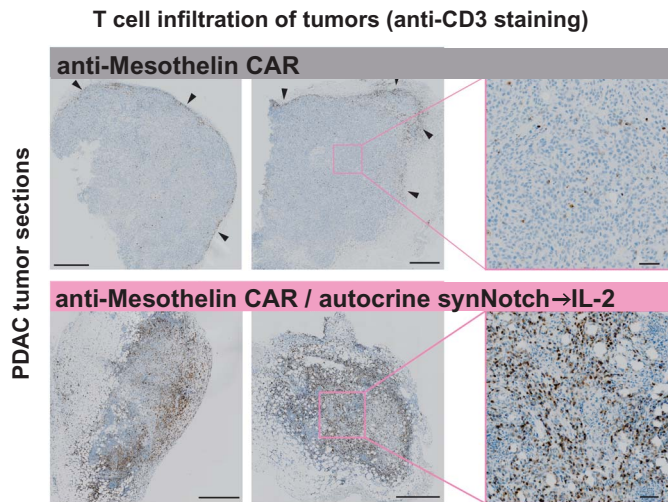
substantially increased infiltration of T cells throughout the tumor core (Fig. 4, bottom). A similar infiltration and expansion of the CD8⁺ lymphocytes also seen in B16-F10 OVA melanoma tumors sampled 10 days after treatment with OT-1 T cells bearing the synthetic IL-2 circuit (fig. S12A).

To profile the tumors in more detail, we performed flow cytometry and Cytometry by time

Fig. 4. The synthetic IL-2 circuit enables T cell infiltration into immune-excluded tumors. KPC CD19⁺

tumors were engrafted subcutaneously, treated with engineered T cells, and analyzed by IHC for T cell infiltration (anti-CD3 stain). Anti-mesothelin CAR T cells (top) failed to penetrate into the tumor and only infiltrated the tumor edges (black arrows). Addition of synthetic autocrine IL-2 circuit (bottom) resulted in

substantially increased T cell infiltration into tumor core. Tumors were collected 23 days (left) and 8 days (center) after T cell injection. Zoomed out scale bars are 500 μ m, zoomed in are 50 μ m.



of flight (CyTOF) analyses on excised and dissociated tumors. To track the endogenous (host) T cells independently from the adoptively transferred CAR T cells, we adoptively transferred congenic Thy1.1 or CD45.1 CAR T cells into Thy1.2 or CD45.2 mice, respectively, allowing us to clearly distinguish endogenous from transplanted T cells by flow cytometry.

These studies showed that the engineered autocrine T cells (expressing both CAR and the synNotch \rightarrow IL-2 circuit) drove substantial intratumoral infiltration of both adoptively transferred (engineered) T cells and native host T cells (Fig. 5A and fig. S12B). By contrast parallel analysis of tumors treated with the paracrine synNotch \rightarrow IL-2 circuit (CAR and synthetic cytokine circuit are expressed by two separate, co-injected cell types) showed expansion of native T cells only and no expansion of the adoptively transferred CAR T cells (Fig. 5A and fig. S13B), suggesting that in the paracrine configuration, induced IL-2 was primarily consumed by competing native T cells, leaving little available to drive expansion of the rarer CAR T cells.

Unsupervised clustering (41) of the CyTOF measurements (from the CD45⁺ immune cell infiltrate in KPC tumors) identified the primary therapeutic effect of the autocrine IL-2 circuit as enrichment of the population of activated adoptively transferred CAR T cells (Fig. 5B). Little change was seen in the myeloid compartments (42), suggesting that synthetic IL-2 production acts primarily to drive T cell infiltration (both native and adoptive) and not by altering myeloid cell-associated immune suppression. Furthermore, the expansion of T cells was completely constrained to the tumor as no changes were seen in immune cells from isolated spleens by flow cytometry or CyTOF analysis (figs. S12A and S16), highlight-

ing the focused local activity of the engineered cytokine circuit.

In addition to driving expansion of cytotoxic T cells in these immunologically cold tumors, the synthetic autocrine IL-2 circuit improved the phenotypes of the CAR T cells that infiltrate the tumor. CyTOF analysis showed that the synthetic autocrine IL-2 circuit up-regulated markers of T cell activation (CD25), effector activity (Granzyme B) and proliferation (Ki67). Conversely, these IL-2-enhanced T cells also showed reduced expression of markers of exhaustion (Tim3, Lag3, PD-1) (Fig. 5C and fig. S14B) (43). Most native T cells (non-CAR) found in the tumors, however, appear to act simply as IL-2 sinks—they did not show markers of activation, effector function, proliferation, or exhaustion (Fig. 5C and fig. S14B) but instead largely exhibited a naïve phenotype (fig. S14, C and D, and fig. S15C). The phenotype of the regulatory T cell population was mostly unchanged (figs. S14D and S15D). These findings suggest that the tumor has a significant population of native host T cells that, in bulk, compete to consume IL-2 without contributing to the antitumor response (akin to T_{reg} suppression through IL-2 consumption).

Discussion

Cell-delivered IL-2 is a powerful tool to synergize with therapeutic T cells

Cytokines such as IL-2 have long been known as powerful stimulators of antitumor immunity (44). However, systemic IL-2 delivery is also well known to be highly toxic, leading to a broad set of adverse effects such as capillary leak syndrome, thereby greatly limiting its therapeutic use (45). Most current efforts in IL-2 engineering have focused on engineering the cytokine to be more selective for tumors,

but we employ a different strategy: harnessing the power of an engineered cell to identify a tumor and locally deliver IL-2 exactly where it is needed. We show that cell-mediated local cytokine (IL-2) delivery can effectively overcome immune suppression, augmenting CAR T cells to efficiently clear multiple immune-excluded tumor models (pancreatic cancer and melanoma) that are otherwise nearly completely resistant to standard CAR T cell treatment.

However, the exact manner by which the cytokine is produced is critical to its success. First, cytokine production must be dynamically regulated (inducible). Constant production of IL-2 risks exacerbating off-target toxicity. Moreover, constitutive IL-2 expression in T cells has negative effects as it leads to terminal differentiation, fails to drive autonomous proliferation, and is limited by payload silencing. Second, to bypass TCR/CAR suppression by the tumor microenvironment induction of IL-2 production must be independent of the TCR activation pathway (e.g., NFAT promoter-induced IL-2 still requires TCR/CAR activation to be triggered). We find that one powerful solution to this constraint is to engineer a synthetic signal transduction pathway that is tumor-triggered but bypasses the native CAR/TCR activation pathway (Fig. 6, A and B). Use of a synNotch receptor that detects the tumor to drive IL-2 production provides a simple and modular way to achieve this goal. The synNotch IL-2 circuit can maintain payload expression despite T cell inhibition or exhaustion (fig. S17A).

Finally, we find that simply having an immune cell that can individually produce high levels of IL-2 in the tumor is not sufficient to overcome suppression. The specific circuit architecture is critical, including exactly which cells produce IL-2. We find that an effective therapeutic response is only observed with an autocrine IL-2 circuit (i.e., the synthetic IL-2 induction pathway is contained within the same cell as the antitumor CAR/TCR).

Mechanisms underlying autocrine/paracrine circuit differences

Why does the autocrine IL-2 induction circuit perform so much better than the equivalent paracrine circuit in driving T cell infiltration of immunosuppressed tumor models? Both circuits act by the same principle of delivering high levels of IL-2 (fig. S17B) directly to the tumor. Moreover, we also ask why we only see this large difference in autocrine versus paracrine circuit efficacy in the presence of a native immune system.

It is likely that there are multiple mechanisms that contribute to the far better efficacy of the autocrine circuit (Fig. 6, C and D). These mechanisms are tightly interlinked and likely act in a highly cooperative manner, thus making

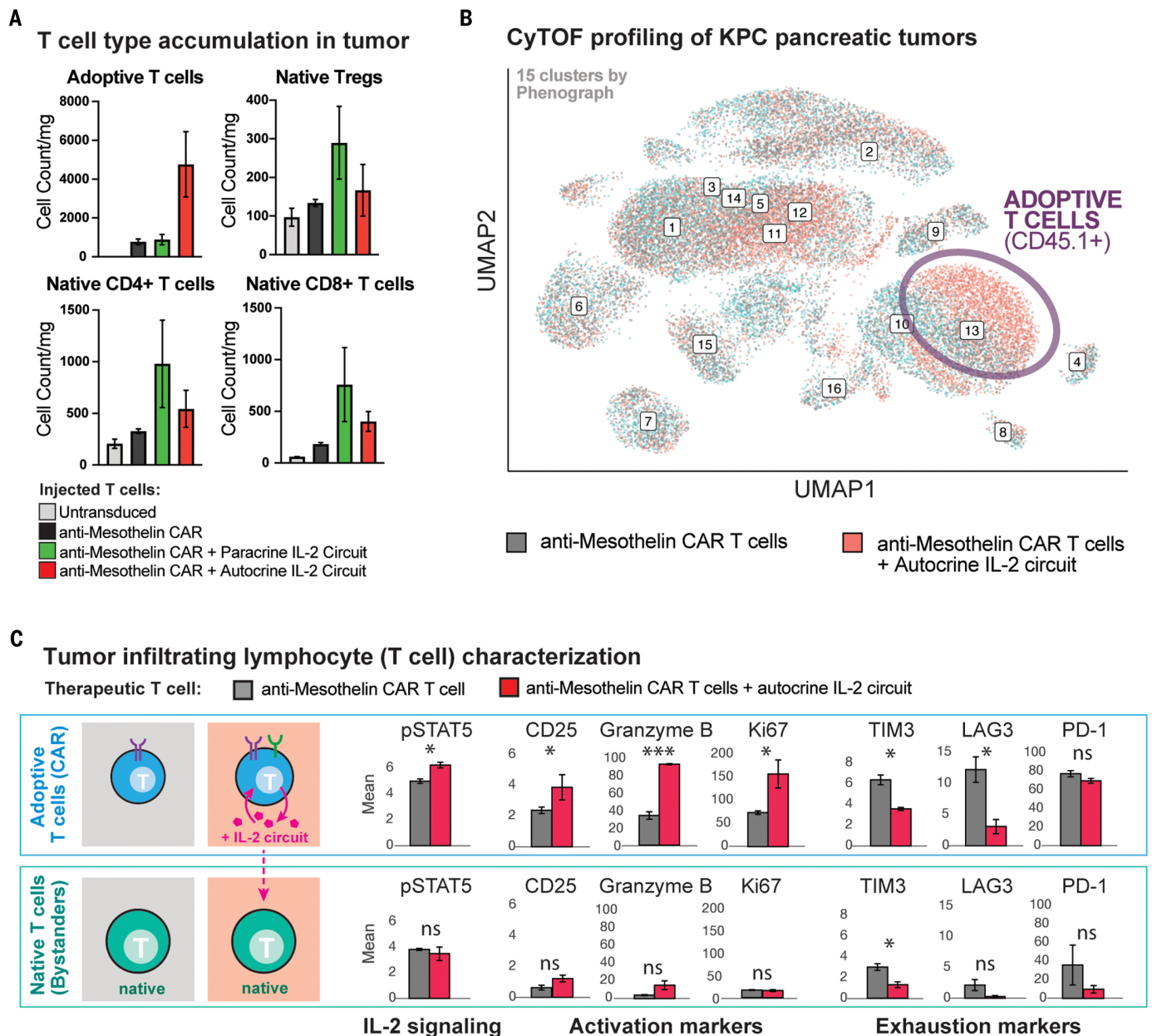


Fig. 5. Profiling of the tumor microenvironment shows expansion and activation of CAR T cells with the autocrine IL-2 circuit. (A) Treated KPC CD19⁺ tumors were collected as in Fig. 4 after 9 days for analysis by CyTOF using CD45.1 as a marker of adoptively transferred T cells and CD45.2 as marker of native T cells. Native T cells and regulatory T cells (T_{regs}) showed expansion in tumors treated with anti-mesothelin CAR + synthetic IL-2 circuit in autocrine or paracrine configuration whereas adoptive (CAR) T cells showed far more substantial expansion only with anti-mesothelin CAR + synthetic IL-2 circuit in autocrine configuration. $n = 3$ samples per treatment, no P value calculated. Counts are normalized to tumor weight. (B) Unsupervised analysis of CyTOF data. UMAP shown for KPC tumors treated by anti-mesothelin CAR \pm IL-2 circuit (autocrine). Labeled numbers indicate clusters by phenograph. Enrichment was only seen in adoptively transferred CAR

T cells when the synthetic IL-2 circuit was engaged, see fig. S13 for mean marker expression for each phenograph cluster and measures of cluster enrichment. (C) Analysis of tumor-infiltrating lymphocytes markers in CAR T cells (CD45.1) from CyTOF data shows that CAR T cells with the synthetic IL-2 circuit in autocrine show higher expression of markers of IL-2 signaling (pSTAT5), activation (CD25), effector function (Granzyme B), and proliferation (Ki67), while showing decreased expression of markers of exhaustion (Tim3, Lag3, PD1). Matched analysis of native T cells (CD45.2) shows limited IL-2 signaling, activation, effector responses, proliferation, or exhaustion markers, with or without addition of the synthetic IL-2 circuit. Mean \pm S.D. is plotted. See figs. S13 to S15, for additional data including repeat CyTOF runs. Statistical significance was tested using a two-tailed Student's t test. (n.s., not significant > 0.05 , * $P < 0.05$, *** $P < 0.001$).

it difficult to precisely pinpoint the relative contribution of each mechanism.

First, it is likely that autocrine cells have preferential access to self-produced IL-2, especially in environments with competing IL-2

sinks. Paracrine circuits must physically transfer IL-2 further through space from a producer T cell to an effector T cell. This becomes challenging in the presence of competing IL-2 consumer cells (e.g., T_{regs} in immune competent

models), which can greatly reduce the effective length scale of IL-2 signaling, creating gradients that drop off sharply around IL-2 sources (46). Here, in both the autocrine and paracrine circuit we observe an expansion of host T_{reg} cells

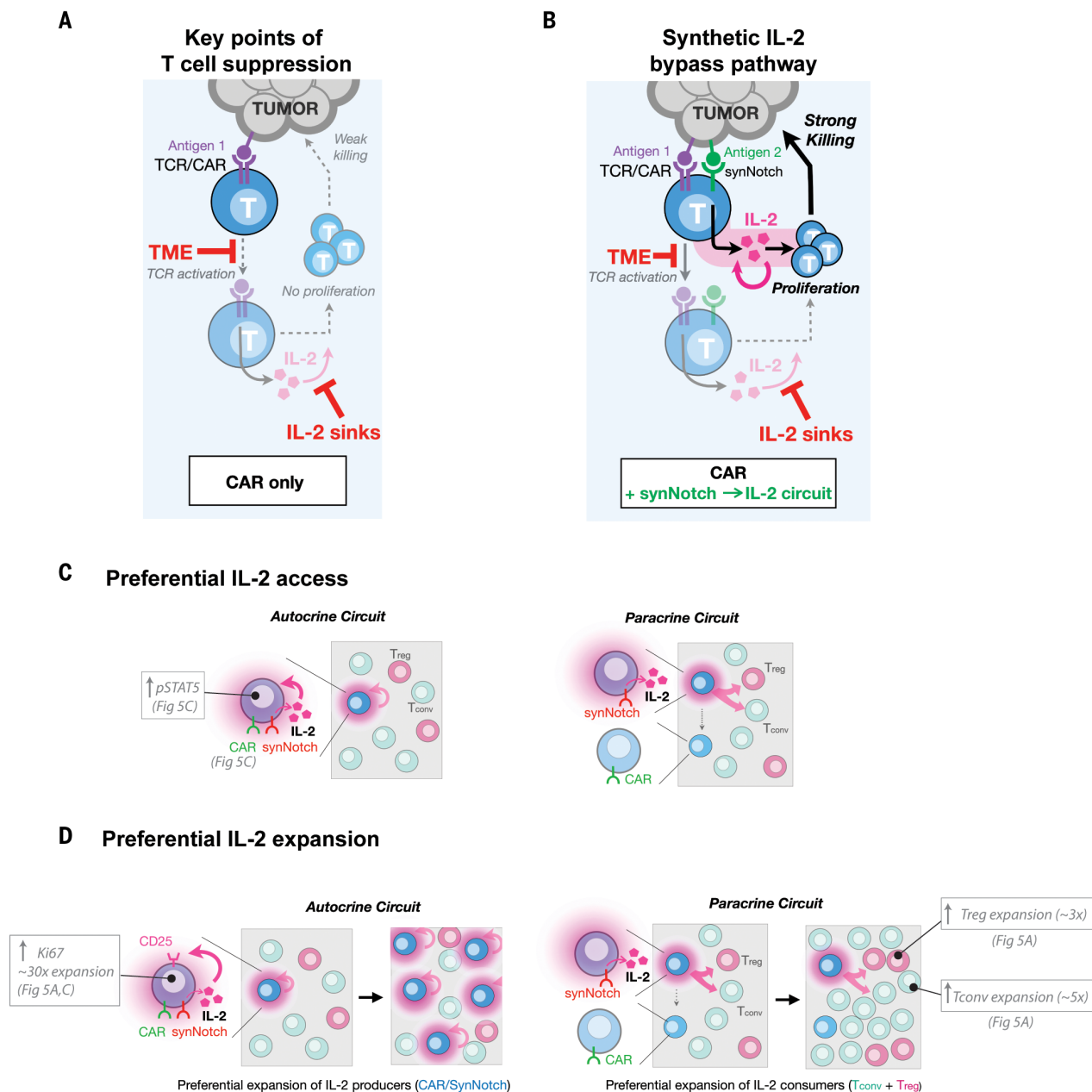


Fig. 6. Bypassing tumor immune suppression mechanisms with a synthetic IL-2 delivery circuit. (A) Standard CAR/TCR T cell activity in suppressive microenvironments is limited by inhibition of T cell activation, minimal production of IL-2, and consumption of IL-2 by competing native cells (sinks). Activation of both TCR and cytokine signaling, required for the full T cell response (AND gate), is blocked at these steps. (B) Creating a bypass channel for IL-2 production that is independent of CAR/TCR activation can overcome key suppressive steps. New circuits allow initiation of T cell activation through synergistic TCR/cytokine stimulation, leading to positive feedback, T cell activation, proliferation, and efficient killing of tumor cells. The synthetic circuit reconstitutes the

key requirements for a strong T cell response in a manner that bypasses key suppressive bottlenecks. (C) Schematic differences between autocrine and paracrine IL-2 signaling in the presence of IL-2 consumers. An autocrine IL-2 circuit provides preferential spatial access to self-made IL-2 in comparison to a paracrine IL-2 circuit, where CAR T cells must compete with other IL-2 consumers (Tregs or T-naive cells). (D) An autocrine IL-2 leads to preferential expansion of IL-2 producers (through T cell activation and up-regulation of CD25), by contrast to a paracrine circuit in which IL-2 producers compete on equal or lesser footing with IL-2 consumers and are not selectively enriched limiting total IL-2 produced and failing to accumulate enough IL-2 to overcome thresholds required for T cell activation.

(Fig. 5A and fig. S15A); however, we also see a much larger expansion of naïve T cells (figs. S12B and S15A). These results suggest that host conventional T cells in the tumor can also play a significant role as IL-2 sinks, especially given their vast excess population. Although it

is difficult to parse out the relative contribution of these Tregs versus conventional T cells as IL-2 consumers, it is not uncommon to observe the presence of large numbers of tumor-infiltrating but non-tumor-reactive T cells (30). Whatever their relative contribution,

both of these IL-2 consumers are expected to decrease the effective signaling distance of IL-2 producers (47, 48), which would strongly favor the efficacy of autocrine over paracrine IL-2 production in driving CAR T cell expansion.

Second, it is also likely that autocrine cells are capable of preferential expansion in response to the available pool of IL-2. There is a characteristic proliferative positive feedback loop that could in principle take place with T cells that can induce both IL-2 and TCR/CAR activation. T cell activation can both trigger an initially IL-2-independent proliferative response (49) and induce expression of the high-affinity IL-2 receptor subunit CD25 (fig. S17C), which allows T cells to outcompete other T cells for available IL-2. Because an autocrine circuit cell contains both the CAR and synNotch→IL-2 circuit, it has the capability to become both a preferred IL-2 responder (through T cell activation) and strong IL-2 producer (through synNotch activation) within a tumor. We hypothesize that these dually activated autocrine cells could thereby initiate a powerful population-level positive feedback loop that builds up even higher levels of intratumoral IL-2 as a result of preferential expansion of better IL-2 consumers/responders. This population-positive feedback would not take place in the paracrine circuit, as the IL-2 producers do not up-regulate CD25 (fig. S17C) and their IL-2 production would largely contribute to expanding competing T cells (such as T_{regs}) that act to suppress T cell-based immunity. Several pieces of evidence support this model of preferred expansion of autocrine circuit cells. First, only in the autocrine CAR T cells do we observe significantly higher expression of the proliferation marker Ki67 (Fig. 5C and fig. S14B). Second, we do not see increased tumor control with an autocrine circuit that produces the homeostatic cytokine IL-7 (fig. S17D). Further experiments will be needed to definitively evaluate the relative contributions of the multiple mechanisms discussed in this model.

Essential requirements to bypass tumor immunosuppression

Our efforts to systematically design CAR T circuits that couple IL-2 production/signaling with CAR signaling in alternative ways also elucidates the basic design principles of native T cell activation. The T cell system has evolved to severely restrict improper activation while simultaneously being able to launch a locally explosive response once triggered. Population-level positive feedback signaling using a shared cytokine (IL-2) allows this type of digital response between on and off states (50, 51). In this model, T cells must not only be stimulated by the proper antigens but must also subsequently produce enough IL-2 to overcome the threshold set by competing IL-2 consumer cells present throughout the microenvironment (52). This control mechanism, however, provides weak points that tumors can take advantage of for immune suppression. Many tumors keep a strong T cell response in check,

either by blocking T cell activation (28) or increasing competition for amplification factors such as IL-2.

Here we show that it is possible to still reconstitute the pathways required for a strong antitumor T cell response (i.e., rewiring the cell such that T cell activation, co-stimulation, and IL-2 signaling are still cooperatively stimulated), but in a way that now evades the major tumor suppressive mechanisms. Normally IL-2 is produced after T cell activation and acts as a critical amplifier of T cell activity. By placing IL-2 production under the control of a new TCR-independent but still tumor-targeted synthetic receptor we can now produce IL-2 immediately and consistently after tumor entry despite suppression of T cell activation. In addition, IL-2 consumers normally apply a selective pressure only allowing strongly activated effector T cells to expand (52). By coupling TCR/CAR activation and synNotch-driven IL-2 production in an autocrine IL-2 circuit, we can selectively expand the engineered therapeutic T cell population out of a background of competing IL-2 consumers. These rewired cells ultimately activate the same critical pathways (TCR and IL-2 pathways) as seen in native T cell responses but do so in a different temporal order and in response to different inputs allowing them to be far more effective in tumor-targeted therapy (Fig. 6). The engineered circuit maintains the explosive cell expansion necessary for robust antitumor activity but triggered in a manner that evades the major mechanisms of immunosuppression.

The power of alternatively wired immune cell circuits

In summary, we have been able to use flexible synthetic biology tools—such as the synNotch receptor system—to create new, alternative ways to rapidly establish both the TCR and IL-2 pathway activity required for an effective and sustained T cell response. The resulting bypass channel for IL-2 production allows for improved tumor control and reduced toxicity compared to alternative mechanisms of IL-2 delivery. Synthetic cytokine production circuits may represent a general solution for engineering immune cell therapies that can function more effectively in hostile tumor microenvironments, illustrating the power of customizing immune responses in highly precise but novel ways.

REFERENCES AND NOTES

- S. J. Schuster *et al.*, Tisagenlecleucel in Adult Relapsed or Refractory Diffuse Large B-Cell Lymphoma. *N. Engl. J. Med.* **380**, 45–56 (2019). doi: [10.1056/NEJMoa1804980](https://doi.org/10.1056/NEJMoa1804980); pmid: [30501490](https://pubmed.ncbi.nlm.nih.gov/30501490/)
- N. C. Munshi *et al.*, Idecabtagene Vicleucel in Relapsed and Refractory Multiple Myeloma. *N. Engl. J. Med.* **384**, 705–716 (2021). doi: [10.1056/NEJMoa2024850](https://doi.org/10.1056/NEJMoa2024850); pmid: [33626253](https://pubmed.ncbi.nlm.nih.gov/33626253/)
- A. R. Haas *et al.*, Phase I Study of Lentiviral-Transduced Chimeric Antigen Receptor-Modified T Cells Recognizing Mesothelin in

- Advanced Solid Cancers. *Mol. Ther.* **27**, 1919–1929 (2019). doi: [10.1016/j.jymthe.2019.07.015](https://doi.org/10.1016/j.jymthe.2019.07.015); pmid: [31420241](https://pubmed.ncbi.nlm.nih.gov/31420241/)
- S. Mariathasan *et al.*, TGF β attenuates tumour response to PD-L1 blockade by contributing to exclusion of T cells. *Nature* **554**, 544–548 (2018). doi: [10.1038/nature25501](https://doi.org/10.1038/nature25501); pmid: [29443960](https://pubmed.ncbi.nlm.nih.gov/29443960/)
- A. Xia, Y. Zhang, J. Xu, T. Yin, X.-J. Lu, T Cell Dysfunction in Cancer Immunity and Immunotherapy. *Front. Immunol.* **10**, 1719 (2019). doi: [10.3389/fimmu.2019.01719](https://doi.org/10.3389/fimmu.2019.01719); pmid: [31379886](https://pubmed.ncbi.nlm.nih.gov/31379886/)
- A. B. Frey, N. Monu, Signaling defects in anti-tumor T cells. *Immunol. Rev.* **222**, 192–205 (2008). doi: [10.1111/j.1600-065X.2008.00606.x](https://doi.org/10.1111/j.1600-065X.2008.00606.x); pmid: [18364003](https://pubmed.ncbi.nlm.nih.gov/18364003/)
- M. Y. Balkhi, Q. Ma, S. Ahmad, R. P. Jurghans, T cell exhaustion and Interleukin 2 downregulation. *Cytokine* **71**, 339–347 (2015). doi: [10.1016/j.cyt.2014.11.024](https://doi.org/10.1016/j.cyt.2014.11.024); pmid: [25516298](https://pubmed.ncbi.nlm.nih.gov/25516298/)
- L. Tang *et al.*, Enhancing T cell therapy through TCR-signaling-responsive nanoparticle drug delivery. *Nat. Biotechnol.* **36**, 707–716 (2018). doi: [10.1038/nbt.4181](https://doi.org/10.1038/nbt.4181); pmid: [29985479](https://pubmed.ncbi.nlm.nih.gov/29985479/)
- L. Zhang *et al.*, Tumor-infiltrating lymphocytes genetically engineered with an inducible gene encoding interleukin-12 for the immunotherapy of metastatic melanoma. *Clin. Cancer Res.* **21**, 2278–2288 (2015). doi: [10.1158/1078-0432.CCR-14-2085](https://doi.org/10.1158/1078-0432.CCR-14-2085); pmid: [25695689](https://pubmed.ncbi.nlm.nih.gov/25695689/)
- M. B. Atkins *et al.*, High-dose recombinant interleukin 2 therapy for patients with metastatic melanoma: Analysis of 270 patients treated between 1985 and 1993. *J. Clin. Oncol.* **17**, 2105–2116 (1999). doi: [10.1200/JCO.1999.17.7.2105](https://doi.org/10.1200/JCO.1999.17.7.2105); pmid: [10561265](https://pubmed.ncbi.nlm.nih.gov/10561265/)
- Q. Zhang *et al.*, A human orthogonal IL-2 and IL-2R β system enhances CAR T cell expansion and antitumor activity in a murine model of leukemia. *Sci. Transl. Med.* **13**, eabg6986 (2021). doi: [10.1126/scitranslmed.abg6986](https://doi.org/10.1126/scitranslmed.abg6986); pmid: [34936380](https://pubmed.ncbi.nlm.nih.gov/34936380/)
- L. Morsut *et al.*, Engineering Customized Cell Sensing and Response Behaviors Using Synthetic Notch Receptors. *Cell* **164**, 780–791 (2016). doi: [10.1016/j.cell.2016.01.012](https://doi.org/10.1016/j.cell.2016.01.012); pmid: [26830878](https://pubmed.ncbi.nlm.nih.gov/26830878/)
- K. T. Roybal *et al.*, Precision Tumor Recognition by T Cells With Combinatorial Antigen-Sensing Circuits. *Cell* **164**, 770–779 (2016). doi: [10.1016/j.cell.2016.01.011](https://doi.org/10.1016/j.cell.2016.01.011); pmid: [26830879](https://pubmed.ncbi.nlm.nih.gov/26830879/)
- K. A. Smith, Interleukin-2: Inception, impact, and implications. *Science* **240**, 1169–1176 (1988). doi: [10.1126/science.3131876](https://doi.org/10.1126/science.3131876); pmid: [3131876](https://pubmed.ncbi.nlm.nih.gov/3131876/)
- Z. Sun *et al.*, A next-generation tumor-targeting IL-2 preferentially promotes tumor-infiltrating CD8⁺ T-cell response and effective tumor control. *Nat. Commun.* **10**, 3874 (2019). doi: [10.1038/s41467-019-11782-w](https://doi.org/10.1038/s41467-019-11782-w); pmid: [31462678](https://pubmed.ncbi.nlm.nih.gov/31462678/)
- G. R. Weiss *et al.*, Molecular insights on the peripheral and intratumoral effects of systemic high-dose rIL-2 (aldesleukin) administration for the treatment of metastatic melanoma. *Clin. Cancer Res.* **17**, 7440–7450 (2011). doi: [10.1158/1078-0432.CCR-11-1650](https://doi.org/10.1158/1078-0432.CCR-11-1650); pmid: [21976537](https://pubmed.ncbi.nlm.nih.gov/21976537/)
- M. C. Panelli *et al.*, Gene-expression profiling of the response of peripheral blood mononuclear cells and melanoma metastases to systemic IL-2 administration. *Genome Biol.* **3**, RESEARCH0035 (2002). doi: [10.1186/gb-2002-3-7-research0035](https://doi.org/10.1186/gb-2002-3-7-research0035); pmid: [12184809](https://pubmed.ncbi.nlm.nih.gov/12184809/)
- T. Saito *et al.*, Two FOXP3(+)/CD4(+) T cell subpopulations distinctly control the prognosis of colorectal cancers. *Nat. Med.* **22**, 679–684 (2016). doi: [10.1038/nm.4086](https://doi.org/10.1038/nm.4086); pmid: [2711280](https://pubmed.ncbi.nlm.nih.gov/2711280/)
- M. Ahmadzadeh, S. A. Rosenberg, IL-2 administration increases CD4+ CD25(hi) Foxp3+ regulatory T cells in cancer patients. *Blood* **107**, 2409–2414 (2006). doi: [10.1182/blood-2005-06-2399](https://doi.org/10.1182/blood-2005-06-2399); pmid: [16304057](https://pubmed.ncbi.nlm.nih.gov/16304057/)
- K. Staveley-O'Carroll *et al.*, Induction of antigen-specific T cell anergy: An early event in the course of tumor progression. *Proc. Natl. Acad. Sci. U.S.A.* **95**, 1178–1183 (1998). doi: [10.1073/pnas.95.3.1178](https://doi.org/10.1073/pnas.95.3.1178); pmid: [9448305](https://pubmed.ncbi.nlm.nih.gov/9448305/)
- A. M. Levin *et al.*, Exploiting a natural conformational switch to engineer an interleukin-2 'superkine'. *Nature* **484**, 529–533 (2012). doi: [10.1038/nature10975](https://doi.org/10.1038/nature10975); pmid: [22446627](https://pubmed.ncbi.nlm.nih.gov/22446627/)
- D. L. Wallace *et al.*, Prolonged exposure of naive CD8+ T cells to interleukin-7 or interleukin-15 stimulates proliferation without differentiation or loss of telomere length. *Immunology* **119**, 243–253 (2006). doi: [10.1111/j.1365-2567.2006.02429.x](https://doi.org/10.1111/j.1365-2567.2006.02429.x); pmid: [17005004](https://pubmed.ncbi.nlm.nih.gov/17005004/)
- L. V. Hurlton *et al.*, Tethered IL-15 augments antitumor activity and promotes a stem-cell memory subset in tumor-specific T cells. *Proc. Natl. Acad. Sci. U.S.A.* **113**, E7788–E7797 (2016). doi: [10.1073/pnas.1610544113](https://doi.org/10.1073/pnas.1610544113); pmid: [27849617](https://pubmed.ncbi.nlm.nih.gov/27849617/)
- P. F. Robbins *et al.*, Single and dual amino acid substitutions in TCR CDRs can enhance antigen-specific T cell functions. *J. Immunol.* **180**, 6116–6131 (2008). doi: [10.4049/jimmunol.180.9.6116](https://doi.org/10.4049/jimmunol.180.9.6116); pmid: [18424733](https://pubmed.ncbi.nlm.nih.gov/18424733/)

25. P. F. Robbins *et al.*, A pilot trial using lymphocytes genetically engineered with an NY-ESO-1-reactive T-cell receptor: Long-term follow-up and correlates with response. *Clin. Cancer Res.* **21**, 1019–1027 (2015). doi: [10.1158/1078-0432.CCR-14-2708](https://doi.org/10.1158/1078-0432.CCR-14-2708); pmid: [25538264](https://pubmed.ncbi.nlm.nih.gov/25538264/)
26. J. Z. Williams *et al.*, Precise T cell recognition programs designed by transcriptionally linking multiple receptors. *Science* **370**, 1099–1104 (2020). doi: [10.1126/science.abc6270](https://doi.org/10.1126/science.abc6270); pmid: [33243890](https://pubmed.ncbi.nlm.nih.gov/33243890/)
27. C. C. Kloss, M. Condomines, M. Cartellieri, M. Bachmann, M. Sadelain, Combinatorial antigen recognition with balanced signaling promotes selective tumor eradication by engineered T cells. *Nat. Biotechnol.* **31**, 71–75 (2013). doi: [10.1038/nbt.2459](https://doi.org/10.1038/nbt.2459); pmid: [23242161](https://pubmed.ncbi.nlm.nih.gov/23242161/)
28. G. P. Mogol *et al.*, Exhaustion-associated regulatory regions in CD8⁺ tumor-infiltrating T cells. *Proc. Natl. Acad. Sci. U.S.A.* **114**, E2776–E2785 (2017). doi: [10.1073/pnas.1620498114](https://doi.org/10.1073/pnas.1620498114); pmid: [28283662](https://pubmed.ncbi.nlm.nih.gov/28283662/)
29. T. Chinen *et al.*, An essential role for the IL-2 receptor in T_{reg} cell function. *Nat. Immunol.* **17**, 1322–1333 (2016). doi: [10.1038/ni.3540](https://doi.org/10.1038/ni.3540); pmid: [27595233](https://pubmed.ncbi.nlm.nih.gov/27595233/)
30. G. Oliveira *et al.*, Phenotype, specificity and avidity of antitumour CD8⁺ T cells in melanoma. *Nature* **596**, 119–125 (2021). doi: [10.1038/s41586-021-03704-y](https://doi.org/10.1038/s41586-021-03704-y); pmid: [34290406](https://pubmed.ncbi.nlm.nih.gov/34290406/)
31. J. Li *et al.*, Tumor Cell-Intrinsic Factors Underlie Heterogeneity of Immune Cell Infiltration and Response to Immunotherapy. *Immunity* **49**, 178–193.e7 (2018). doi: [10.1016/j.immuni.2018.06.006](https://doi.org/10.1016/j.immuni.2018.06.006); pmid: [29958801](https://pubmed.ncbi.nlm.nih.gov/29958801/)
32. S. R. Hingorani *et al.*, Trp53R172H and KrasG12D cooperate to promote chromosomal instability and widely metastatic pancreatic ductal adenocarcinoma in mice. *Cancer Cell* **7**, 469–483 (2005). doi: [10.1016/j.ccr.2005.04.023](https://doi.org/10.1016/j.ccr.2005.04.023); pmid: [15894267](https://pubmed.ncbi.nlm.nih.gov/15894267/)
33. T. N. D. Pham *et al.*, Preclinical Models of Pancreatic Ductal Adenocarcinoma and Their Utility in Immunotherapy Studies. *Cancers* **13**, 440 (2021). doi: [10.3390/cancers13030440](https://doi.org/10.3390/cancers13030440); pmid: [33503832](https://pubmed.ncbi.nlm.nih.gov/33503832/)
34. I. M. Stromnes *et al.*, T Cells Engineered against a Native Antigen Can Surmount Immunologic and Physical Barriers to Treat Pancreatic Ductal Adenocarcinoma. *Cancer Cell* **28**, 638–652 (2015). doi: [10.1016/j.ccell.2015.09.022](https://doi.org/10.1016/j.ccell.2015.09.022); pmid: [26525103](https://pubmed.ncbi.nlm.nih.gov/26525103/)
35. M. K. Gately, T. D. Anderson, T. J. Hayes, Role of asialo-GM1-positive lymphoid cells in mediating the toxic effects of recombinant IL-2 in mice. *J. Immunol.* **141**, 189–200 (1988). pmid: [3259967](https://pubmed.ncbi.nlm.nih.gov/3259967/)
36. E. Hooijberg, A. Q. Bakker, J. J. Ruizendaal, H. Spits, NFAT-controlled expression of GFP permits visualization and isolation of antigen-stimulated primary human T cells. *Blood* **96**, 459–466 (2000). doi: [10.1182/blood.V96.2.459](https://doi.org/10.1182/blood.V96.2.459); pmid: [10887106](https://pubmed.ncbi.nlm.nih.gov/10887106/)
37. H. Yamaue *et al.*, Enhanced interleukin-2 production in human tumor-infiltrating lymphocytes engineered by 3'-truncated interleukin-2 gene. *J. Immunother. Emphasis Tumor Immunol.* **16**, 262–274 (1994). doi: [10.1097/00002371-199411000-00002](https://doi.org/10.1097/00002371-199411000-00002); pmid: [7881635](https://pubmed.ncbi.nlm.nih.gov/7881635/)
38. Y. Hart *et al.*, Paradoxical signaling by a secreted molecule leads to homeostasis of cell levels. *Cell* **158**, 1022–1032 (2014). doi: [10.1016/j.cell.2014.07.033](https://doi.org/10.1016/j.cell.2014.07.033); pmid: [25171404](https://pubmed.ncbi.nlm.nih.gov/25171404/)
39. Y. Refaeli, L. Van Parijs, C. A. London, J. Tschopp, A. K. Abbas, Biochemical mechanisms of IL-2-regulated Fas-mediated T cell apoptosis. *Immunity* **8**, 615–623 (1998). doi: [10.1016/S1074-7613\(00\)80566-X](https://doi.org/10.1016/S1074-7613(00)80566-X); pmid: [9620682](https://pubmed.ncbi.nlm.nih.gov/9620682/)
40. M. E. Pipkin *et al.*, Interleukin-2 and inflammation induce distinct transcriptional programs that promote the differentiation of effector cytolytic T cells. *Immunity* **32**, 79–90 (2010). doi: [10.1016/j.immuni.2009.11.012](https://doi.org/10.1016/j.immuni.2009.11.012); pmid: [20096607](https://pubmed.ncbi.nlm.nih.gov/20096607/)
41. J. H. Levine *et al.*, Data-Driven Phenotypic Dissection of AML Reveals Progenitor-like Cells that Correlate with Prognosis. *Cell* **162**, 184–197 (2015). doi: [10.1016/j.cell.2015.05.047](https://doi.org/10.1016/j.cell.2015.05.047); pmid: [26095251](https://pubmed.ncbi.nlm.nih.gov/26095251/)
42. M. T. Saug *et al.*, Targeting myeloid-inflamed tumor with anti-CSF-1R antibody expands CD137⁺ effector T-cells in the murine model of pancreatic cancer. *J. Immunother. Cancer* **6**, 118 (2018). doi: [10.1186/s40425-018-0435-6](https://doi.org/10.1186/s40425-018-0435-6); pmid: [30424804](https://pubmed.ncbi.nlm.nih.gov/30424804/)
43. Y. Liu *et al.*, IL-2 regulates tumor-reactive CD8⁺ T cell exhaustion by activating the aryl hydrocarbon receptor. *Nat. Immunol.* **22**, 358–369 (2021). doi: [10.1038/s41590-020-00850-9](https://doi.org/10.1038/s41590-020-00850-9); pmid: [33432230](https://pubmed.ncbi.nlm.nih.gov/33432230/)
44. S. A. Rosenberg, IL-2: The first effective immunotherapy for human cancer. *J. Immunol.* **192**, 5451–5458 (2014). doi: [10.4049/jimmunol.1490019](https://doi.org/10.4049/jimmunol.1490019); pmid: [24907378](https://pubmed.ncbi.nlm.nih.gov/24907378/)
45. R. S. Cotran *et al.*, Endothelial activation during interleukin 2 immunotherapy. A possible mechanism for the vascular leak syndrome. *J. Immunol.* **140**, 1883–1888 (1988). doi: [10.4049/jimmunol.140.6.1883](https://doi.org/10.4049/jimmunol.140.6.1883); pmid: [3279124](https://pubmed.ncbi.nlm.nih.gov/3279124/)
46. A. Olyer-Yaniv *et al.*, A Tunable Diffusion-Consumption Mechanism of Cytokine Propagation Enables Plasticity in Cell-to-Cell Communication in the Immune System. *Immunity* **46**, 609–620 (2017). doi: [10.1016/j.immuni.2017.03.011](https://doi.org/10.1016/j.immuni.2017.03.011); pmid: [28389069](https://pubmed.ncbi.nlm.nih.gov/28389069/)
47. K. Thurlay, D. Gerecht, E. Friedmann, T. Höfer, Three-Dimensional Gradients of Cytokine Signaling between T Cells. *PLoS Comput. Biol.* **11**, e1004206 (2015). doi: [10.1371/journal.pcbi.1004206](https://doi.org/10.1371/journal.pcbi.1004206); pmid: [25923703](https://pubmed.ncbi.nlm.nih.gov/25923703/)
48. H. S. Wong *et al.*, A local regulatory T cell feedback circuit maintains immune homeostasis by pruning self-activated T cells. *Cell* **184**, 3981–3997.e22 (2021). doi: [10.1016/j.cell.2021.05.028](https://doi.org/10.1016/j.cell.2021.05.028); pmid: [34157301](https://pubmed.ncbi.nlm.nih.gov/34157301/)
49. W. N. D'Souza, L. Lefrançois, IL-2 is not required for the initiation of CD8 T cell cycling but sustains expansion. *J. Immunol.* **171**, 5727–5735 (2003). doi: [10.4049/jimmunol.171.11.5727](https://doi.org/10.4049/jimmunol.171.11.5727); pmid: [14634080](https://pubmed.ncbi.nlm.nih.gov/14634080/)
50. D. Busse *et al.*, Competing feedback loops shape IL-2 signaling between helper and regulatory T lymphocytes in cellular microenvironments. *Proc. Natl. Acad. Sci. U.S.A.* **107**, 3058–3063 (2010). doi: [10.1073/pnas.0812851107](https://doi.org/10.1073/pnas.0812851107); pmid: [20133667](https://pubmed.ncbi.nlm.nih.gov/20133667/)
51. F. Fuhrmann *et al.*, Adequate immune response ensured by binary IL-2 and graded CD25 expression in a murine transfer model. *eLife* **5**, e20616 (2016). doi: [10.7554/eLife.20616](https://doi.org/10.7554/eLife.20616); pmid: [28035902](https://pubmed.ncbi.nlm.nih.gov/28035902/)
52. T. Höfer, O. Krichevsky, G. Altan-Bonnet, Competition for IL-2 between Regulatory and Effector T Cells to Chisel Immune Responses. *Front. Immunol.* **3**, 268 (2012). doi: [10.3389/fimmu.2012.00268](https://doi.org/10.3389/fimmu.2012.00268); pmid: [22973270](https://pubmed.ncbi.nlm.nih.gov/22973270/)

ACKNOWLEDGMENTS

We thank H. Jiang, E. Collisson, R. Almeida, M.P. Lopez, M. Broecker, Y. Tonai, A. DeGuzman, N. Blizard, and members of the Lim Laboratory and Cell Design Institute for assistance and advice. We acknowledge the PFCC (RRID:SCR_018206) supported in part by Grant NIH P30 DK063720 and by the NIH S10 Instrumentation Grant S10 IS10OD018040-01. **Funding:** This work was supported by the following: Jane Coffin Childs Fellowship (to G.M.A.), NIH K08CA259610 (to G.M.A.), NIH/NIGMS F32 GM120843 (to N.W.F.), Howard Hughes Medical Institute (to W.A.L.), NIH U54CA244438 (to W.A.L.), NIH RO1CA249018 (to W.A.L.), NIH UC4DK116264 (to W.A.L.), NIH U01CA265697 (to W.A.L.) **Author contributions:** Conceptualization: G.M.A., N.W.F., K.C.G., H.E.S., K.T.R., M.S., and W.A.L. Methodology: G.M.A., N.W.F., M.A.Y., H.B., J.Y., and M.S. Investigation: G.M.A., N.W.F., M.A.Y., S.R.S., N.R.R., H.B., M.P., J.L., W.Y., and A.L. Visualization: G.M.A., W.A.L., N.W.F., M.A.Y., N.R.R., and H.B. Funding acquisition: G.M.A. and W.A.L. Project administration: G.M.A. and W.A.L. Supervision: G.M.A., W.A.L., M.S. Writing – G.M.A., N.W.F., W.A.L., N.R.R., H.B. **Competing interests:** W.A.L. holds equity in Gilead Sciences and Intellia Therapeutics, is an adviser for Allogene Therapeutics, and has filed patents related to this work. **Data and materials availability:** All data are available in the manuscript or supplementary materials. Reagents are available from the corresponding author upon reasonable request. Plasmids from this paper will be made available on Addgene. **License information:** Copyright © 2022 the authors, some rights reserved; exclusive licensee American Association for the Advancement of Science. No claim to original US government works. <https://www.sciencemag.org/about/science-licenses-journal-article-reuse>

SUPPLEMENTARY MATERIALS

science.org/doi/10.1126/science.aba1624

Materials and Methods

Figs. S1 to S17

Reference (53)

MDAR Reproducibility Checklist

[View/request a protocol for this paper from Bio-protocol.](#)

Submitted 9 November 2019; resubmitted 19 May 2022

Accepted 21 October 2022

[10.1126/science.aba1624](https://doi.org/10.1126/science.aba1624)